World Journal of Biology Pharmacy and Health Sciences
eISSN: 2582-5542
Cross Ref DOI: 10.30574/wjbphs
Journal homepage: https://wjbphs.com/

(RESEARCH ARTICLE)

Check for updates

Green Synthesis, Characterization and Anti-Bacterial Studies of Copper Oxide Nanoparticles Using *Croton scabiosus* Bedd. Fruit Extract

Yuga Vani Bommichetty * and Savithramma Nataru

Department of Botany, Sri Venkateswara University, Tirupati-517502, India.

World Journal of Biology Pharmacy and Health Sciences, 2026, 26(02), 102-110

Publication history: Received on 31 March 2026; revised on 06 May 2026; accepted on 09 May 2026

Article DOI: https://doi.org/10.30574/wjbphs.2026.26.2.0251

Abstract

The development of eco-friendly, cost-effective methodologies for the biosynthesis of metal oxide nanoparticles represents a primary objective in contemporary green nanoscience. The present study reports the biogenic synthesis of copper oxide nanoparticles (CUONPS) employing the aqueous fruit extract of *Croton scabiosus* Bedd. (Euphorbiaceous). This species is a rare, endemic, and IUCN Vulnerable tree species which can act as both reducing and capping agents for the nanoparticles. 1 mM copper nitrate (Cu $(NO_3)_2$) solution was titrated with the fruit extract in a volume ratio of 4:1 (v/v) at room temperature. The progressive color change from green to dark brown within 24–48 hours confirmed the transition of $Cu^{+}2$ ions and formation of CUONPS, which were subjected to various characterization techniques for confirmation of their physical and chemical properties. UV–Vi's spectroscopy revealed a characteristic absorption peak at 274 nm with an optical band gap of 2.65 eV. FTIR analysis confirmed Cu–O lattice vibrations and phytochemical capping. XRD established a simple cubic crystalline phase. DLS revealed a mean hydrodynamic diameter of 19.3 nm (PDI: 0.329) and zeta potential of −13.2 mV. The CUONPS demonstrated potent antimicrobial activity against Escherichia coli, Pseudomonas aeruginosa, Staphylococcus aureus, and Bacillus subtilis, with maximum zone of inhibition of 42 ± 0.1 mm against S. aureus at 200 µg/mL, but very less activity against fungal strains. Hence, the CUONPS from *C. scabiosus* fruit are potential antibacterial agents against various bacterial strains and can be used in pharmaceutical applications.

Keywords: Copper oxide nanoparticles (CUONPS); Green synthesis; *Croton scabiosus*; Antimicrobial

1. Introduction

Nanotechnology has emerged as one of the most transformative domains in modern science, enabling the design and fabrication of materials with precisely tuned physicochemical properties at the 1–100 nm scale. Nanoparticles exhibit profoundly distinct optical, electrical, catalytic, and biological properties relative to their bulk counterparts, arising from quantum confinement effects and markedly elevated surface-to-volume ratios [1,2]. These attributes have stimulated intensive research across drug delivery, bioimaging, environmental remediation, sensing, and antimicrobial therapy [3].

Among the various metal oxide nanoparticles explored, copper oxide nanoparticles (CuONPs) have attracted considerable scientific interest. A critical distinction exists between metallic copper nanoparticles (Cu^0) and CuONPs: Cu^0-NPs are synthesized under strong reducing, oxygen-free conditions and show surface plasmon resonance at 560–590 nm, while CuONPs form under mild oxidative conditions, absorb in the UV region (250–350 nm), and exhibit superior antimicrobial and photocatalytic properties due to their semiconducting nature (Eg ≈ 1.2–3.0 eV), higher colloidal stability via bio-capping, and capacity to generate reactive oxygen species (ROS) [3,4].

* Corresponding author: Yuga Vani Bommichetty

Conventional physicochemical synthesis routes for CuONPs, including co-precipitation, hydrothermal methods, and chemical vapour deposition which require hazardous reducing chemicals, high energy, and generate toxic effluents [5]. Green synthesis strategies employing plant extracts offer a sustainable alternative: through phytochemicals such as polyphenols, flavonoids, and tannins act as both reducing agents (converting $Cu^{+}2$ to Cu0) and capping agents that stabilize and prevent agglomeration of the synthesized nanoparticles [6, 13].

Croton scabiosus Bedd. is an endemic, deciduous tree of the Euphorbiaceae family, distributed in dry-deciduous forests of Ananthapur, Kadapa, and Nellore districts of Andhra Pradesh, India, categorized as 'Vulnerable' by the IUCN Red List [5]. Bark decoctions are used traditionally for leucorrhea and helminthic infestations [6], while seed extracts serve as antivenomous patches [7]. The genus Croton is a rich source of diterpenes, flavonoids, tannins, and phenolic acids. No prior study has investigated its fruit extract for nanoparticle synthesis. Hence, the present study aimed for the green synthesis of CuONPs using *C. scabiosus* Bedd. fruit extract, with comprehensive characterization and evaluation of antimicrobial activity.

2. Material and Methods

2.1. Plant material collection and extraction

Croton scabiosus Bedd. fruits (Figure 1) were collected in March (spring season) from Polathla Forest Reserve, Pendlimarri Mandal, Y.S.R. Kadapa District, Andhra Pradesh, India, and was authenticated by Department of Botany Herbarium, Sri Venkateswara University, Tirupati. They were washed under running tap water and then with deionized water. After shade- drying, fruits were pulverized to a fine powder. Ten grams of powder were boiled in 100 mL deionized water for 30 minutes, filtered through Whatman No. 1 filter paper, and the filtrate stored at 4°C for further use.

Figure 1 *Croton scabiosus* Bedd. (Euphorbiaceae) - fruit-bearing branch

2.2. Synthesis of CuO nanoparticles

CuONPs were synthesized by combining 80 mL of 1 mM copper (II) nitrate (Cu $(NO_3)_2$) solution with 20 mL of C. scabiosus fruit extract under constant magnetic stirring at room temperature. The colour changed from green to dark brown within 24–48 hours, confirming bio reduction of $Cu^{+}2$ ions to CuO nanoparticles. The suspension was centrifuged at 4000 rpm for 15 minutes. The pellet washed three times with deionized water, transferred to pre-weighed petri plates, and dried in a hot-air oven at 70 °C for 12 hours. The dried CuONPs powder was scraped from the petri plates using a sterile spatula and stored in an airtight glass vial at room temperature for further analysis [8,9].

2.3. Characterization of CuO nanoparticles

The synthesized nanoparticles were elucidated by a suite of complementary analytical techniques. Optical properties were assessed using UV-Visible spectrophotometer (Nanodrop-800) to record the absorption spectrum and identify the surface plasmon resonance (SPR) band. Functional groups were identified using an Alpha BRUKER Transmission FTIR Spectrometer over 400–4000 cm^{-1}. Particle size distribution and zeta potential were measured using a HORIBA SZ- 100 nanoparticle analyser. Surface morphology and elemental composition were analysed by SEM-EDAX (JEOL 6390LA / OXFORD XMXN). HRTEM (JEOL JEM-2100, 200 kV) was used for high-resolution morphological analysis with Selected Area Electron Diffraction (SAED) to determine the size and shape of NPs.

2.4. Antimicrobial activity

Antibacterial activity of CuONPs was evaluated against *Escherichia coli* and *Pseudomonas aeruginosa* (Gram-negative) and *Staphylococcus aureus* and *Bacillus subtilis* (Gram-positive) using the agar well- diffusion method (Bauer et al., 1966) [17]. Actively growing cultures (~10^6 CFU/mL, 20 µL) were swabbed on Muller–Hinton Agar (MHA; Himedia Laboratories). Four wells (6 mm) were bored aseptically; CuONPs suspended in DMSO at 50, 100, 150, and 200 µg/mL were added to the wells. DMSO served as negative control; Gentamicin is positive control. Plates were incubated at 37°C for 24 h. Zones of inhibition (ZOI, mm) are expressed as mean ± SD of three independent experiments [17].

Antifungal activity was evaluated against *Aspergillus niger, Fusarium oxysporum, Macrophomina phaseolina,* and *Sclerotium rolfsii* using the well-diffusion method on Potato Dextrose Agar (PDA; Himedia Laboratories) as described by Balouiri et al., (2016) [18]. Actively growing fungal cultures were streaked on PDA; wells received CuONPs suspensions at 20, 40, 60, and 80 µg/mL. Fluconazole served as the standard. Plates were incubated at 28°C for 72 h and radial growth inhibition was assessed.

3. Results and Discussion

3.1. Synthesis of CuO nanoparticles

Formation of CuONPs was evidenced by a colour change from green to dark brown within 24–48 hours upon mixing *C. scabiosus* fruit extract with 1 mM Cu $(NO_3)_2$ solution. This transition reflects bio-oxidation of $Cu^{+}2$ by phytochemicals to CuO in the presence of dissolved oxygen [12]. Simultaneously, these biomolecules cap the nascent nanoparticles, preventing agglomeration [8, 13]. Unlike metallic Cu^0-NP synthesis, which requires strictly inert conditions, CuO formation is facilitated under ambient oxygen access — a mechanistic advantage of this green synthesis route [3].

3.2. Characterization of CuO nanoparticles

The UV–Vi's spectrum (Figure 2) displayed a characteristic absorption peak at 274 nm, in the UV semiconductor absorption range (250–350 nm). The diagnostic of CuONPs may be due to interband transitions of $Cu^{+}2$ d- band electrons [8,9]. This clearly distinguishes the product as CuO (not metallic Cu^0, which shows SPR at 560– 590 nm [3]. The optical band gap (Eg, Tauc plot) was 2.65 eV, consistent with quantum confinement in nanoscale Cu (bulk Eg ~1.2 eV) and within the reported range for green-synthesised CuONPs (2.5–3.0 eV).

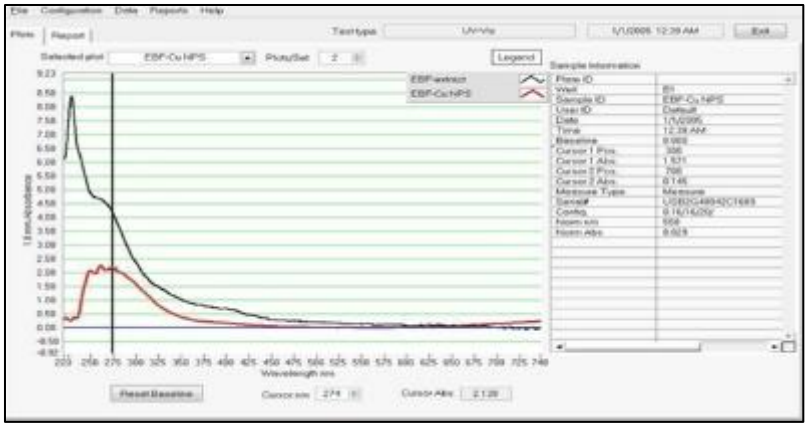

Figure 2 UV–Visible absorption spectrum of CuONPs from *C. scabiosus* Fruit extract

FTIR spectroscopy (Figure 3) identified functional groups on the CuONP surface. The broad absorption band at 3446–3431 cm^{-1} is attributed to O–H stretching of adsorbed phenolic/alcoholic groups from the fruit extract, with N–H contributions from protein-derived capping molecules. The band at 1641–1629 cm^{-1} corresponds to C=C or C=O, Amide I vibrations of flavonoids and aromatic phytochemicals. The band at 1051.24 cm^{-1} is assigned to C–O stretching of carbohydrates and alcohols. Absorption bands below 600 cm^{-1} (notably at 526 cm^{-1}) confirm Cu–O stretching vibrations of the Cu lattice [8]. The presence of phytochemical functional group signatures confirms that polyphenols and flavonoids from *C. scabiosus* serve as effective capping agents, stabilising the CuONPs and preventing agglomeration — consistent with the moderate zeta potential observed.

DLS and zeta potential measurements were performed using the HORIBA SZ-100 nanoparticle analyzer to determine the hydrodynamic particle size distribution and colloidal stability of the biosynthesized CuONPs. The DLS measurement (Figure 4) revealed a single dominant peak with a mean hydrodynamic diameter of 19.3 nm (SD: 11.7 nm, mode: 14.0 nm) and a polydispersity index (PDI) of 0.329, indicating a moderately polydisperse but predominantly nanoscale particle population. Also, the PDI reports the biogenically synthesised CuONPs and is attributed to the heterogeneous nature of the phytochemical capping layer [13]. The Z-average (cumulant) diameter of 3509 nm reflects the presence of larger agglomerated clusters in colloidal suspension, consistent with the aggregation behavior observed in SEM analysis. The scattering light intensity distribution, however, confirms that the primary particle fraction is centered at 19.3 nm, in excellent agreement with crystallite sizes estimated from XRD Scherrer analysis (10–20 nm) and HRTEM measurements.

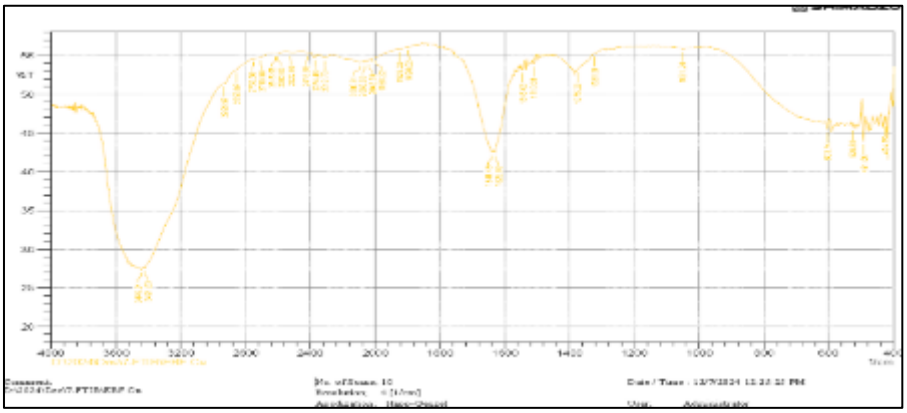

Key peaks: 3446 cm^{-1} (O–H), 1641 cm^{-1} (C=O/C=C), 1051 cm^{-1} (C–O), 526 cm^{-1} (Cu–O).

Figure 3 FTIR spectrum of CuONPs from *Croton scabiosus* Bedd. fruit extract

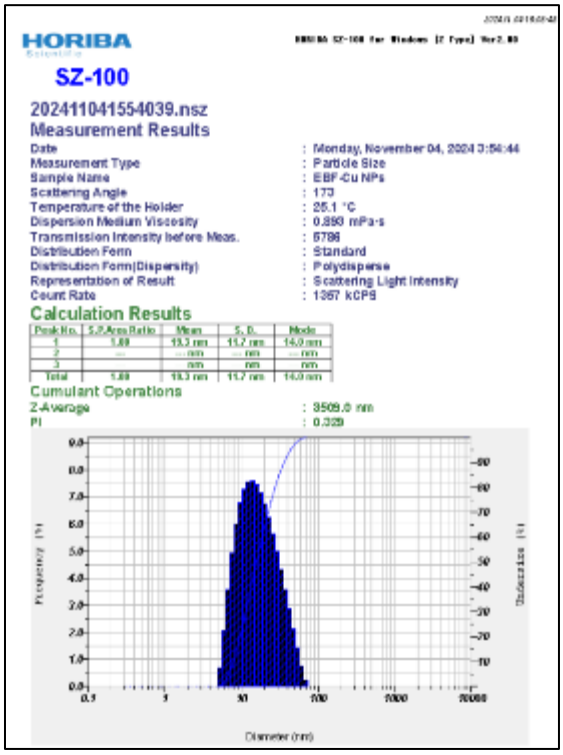

Mean diameter: 19.3 nm; SD: 11.7 nm; PDI: 0.329.

Figure 4 DLS particle size distribution of CuONPs from *C. scabiosus* Fruit extract

The zeta potential of the CuONP colloidal suspension was determined to be −13.2 mV (Figure 5), measured at 25°C with a dispersion conductivity of 1.077 mS/cm. A negative zeta potential in this range indicates moderate electrostatic repulsion between nanoparticles, conferred by the adsorbed phytochemical capping molecules (phenolic hydroxyl, carboxylate, and amide groups) from the *C. scabiosus* fruit extract [11]. While a zeta potential of −13.2 mV suggests moderate rather than maximum colloidal stability (values beyond ±30 mV is considered highly stable), the bio-capping layer provides additional steric stabilization that supplements the electrostatic repulsion. Comparable zeta potential values (−15 to −25 mV) have been reported for green-synthesised CuONPs from other plant sources, with similar particle stabilization attributed to adsorbed phenolics and flavonoids [8, 10].

The EDX spectrum (Figure 6) confirmed the elemental composition of the synthesized CuONPs. Prominent peaks corresponding exclusively to copper (Cu K-series: 62.58 wt%) and oxygen (O K-series: 37.42 wt%) were detected, with no extraneous elemental peaks, validating phase-pure copper oxide synthesis. The XRD pattern (not shown separately) displayed well-resolved diffraction peaks consistent with a simple cubic crystalline phase. The sharp, well-defined peaks confirm high crystallinity. The Scherrer equation yielded crystallite sizes of 10–20 nm, in excellent agreement with DLS (19.3 nm mean) and HRTEM measurements.

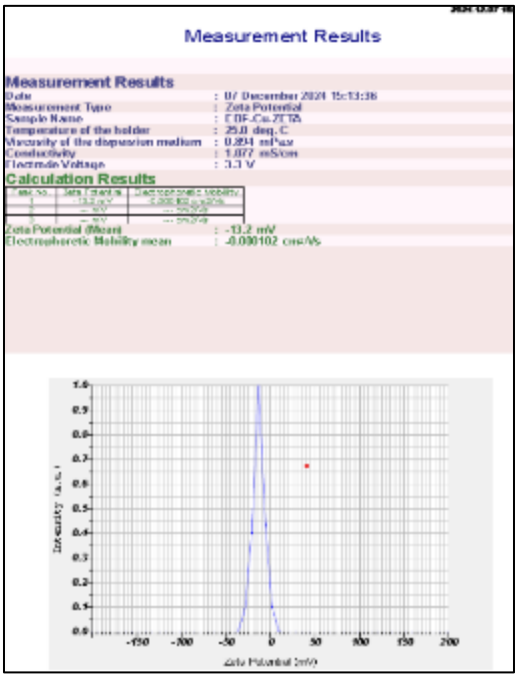

Mean zeta potential: −13.2 mV; electrophoretic mobility: −0.000102 cmZ/Vs.

Figure 5 Zeta potential measurement of CuONPs from *C. scabiosus* Fruit extract

SEM micrographs (Figure 7) were recorded at two magnifications. At low magnification (×1,500; scale bar = 10 µm), a porous, heterogeneous surface architecture with aggregated clusters is visible. At high magnification (×7,000; scale bar = 2 µm), annotated particle dimensions range from 217.59 to 508.70 nm. These SEM-observable aggregates are consistent with the secondary agglomeration behaviour detected by DLS (Z-average: 3509 nm). The primary crystallites, however, are 10–20 nm as established by XRD and DLS.

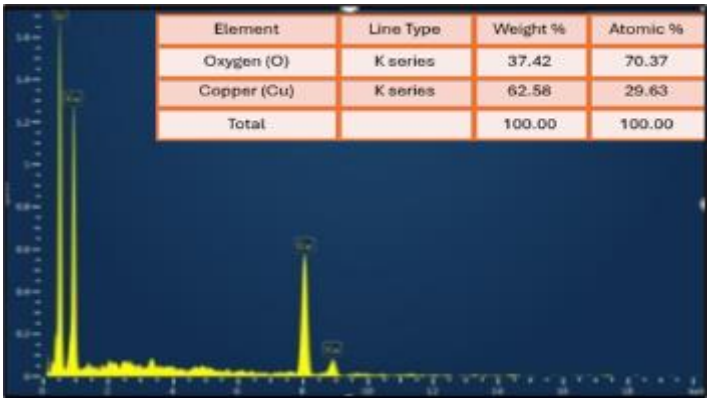

Confirming phase-pure composition (Cu: 62.58 wt%; O: 37.42 wt%).

Figure 6 EDX spectrum and elemental composition of CuONPs from *C. scabiosus* fruit extract

HRTEM analysis (Figure 8) revealed predominantly spherical CuO nanoparticles with well-defined boundaries. Primary particle sizes of 10–20 nm were directly measured from micrographs, in close agreement with EDX and DLS data. The large spherical aggregate (~60–80 nm) visible in the bright-field image represents secondary agglomeration of primary nanocrystallites, consistent with DLS observations. The effective phytochemical capping by *C. scabiosus* fruit constituents restrict primary particle growth while the zeta potential (−13.2 mV) provides moderate electrostatic colloidal stability.

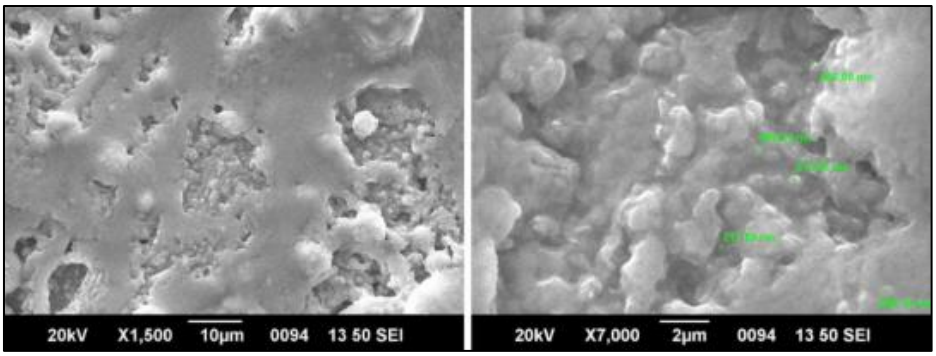

Left: ×1,500 (scale bar = 10 µm); Right: ×7,000 (scale bar = 2 µm) with annotated particle sizes (217–508 nm).

Figure 7 SEM micrographs of CuONPs from *C. scabiosus* Bedd.

3.3. Antimicrobial activity

The antibacterial efficacy of CuONPs against *E. coli, P. aeruginosa* (Gram-negative) and *S.aureus, B. subtilis* (Gram-positive) is presented in Table 1 and Figure 9. Clear, concentrate dependent ZOI were recorded across 50–200 µg/mL. At 200 µg/mL, *S. aureus* showed the largest ZOI (42 ± 0.1 mm), followed by *B. subtilis* (40 ± 0.1 mm), *E. coli* (26 ± 0.1 mm), and *P. aeruginosa* (19 ± 0.1 mm). CuONPs surpassed the gentamicin standard for *S. aureus* (22 ± 0.1 mm) and *B. subtilis* (15 ± 0.1 mm). Gram-positive organisms showed consistently higher susceptibility than Gram-negative bacteria, attributed to the absence of an outer membrane barrier in Gram-positive cell walls [9].

Table 1 Zones of inhibition (mm, mean ± SD) of CuONPs against bacterial pathogens

Conc. (µg/mL)	*E. coli*	*P. aeruginosa*	*S. aureus*	*B. subtilis*
50	11 ± 0.1	10 ± 0.1	26 ± 0.1	20 ± 0.2
100	15 ± 0.1	12 ± 0.2	30 ± 0.1	27 ± 0.1
150	20 ± 0.2	15 ± 0.1	36 ± 0.1	35 ± 0.1
200	26 ± 0.1	19 ± 0.1	42 ± 0.1	40 ± 0.1
Standard	25 ± 0.1	20 ± 0.1	22 ± 0.1	15 ± 0.1

Values are mean ± SD of three independent experiments. Standard: Gentamicin (Himedia Laboratories).

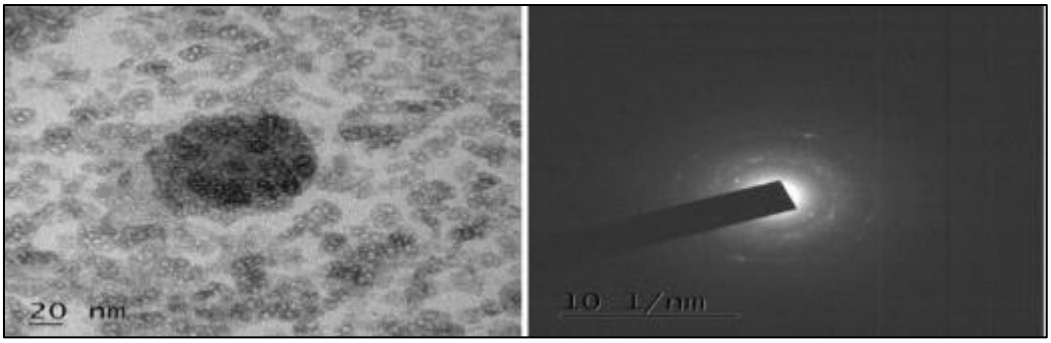

Left: bright field image (scale bar = 20 nm) showing spherical nanocrystallites. Right: SAED pattern (scale bar = 10 1/nm) confirming polycrystalline Cu phase.

Figure 8 HRTEM images of Cu ONPs (JEOL JEM-2100, 200 kV).

The multifaceted antimicrobial mechanism involves: (i) Cu^{+} ion release disrupting cell membrane integrity; (ii) ROS generation (hydroxyl radicals, superoxide, H_2O_2) inducing oxidative stress, lipid peroxidation, DNA fragmentation, and protein denaturation; and (iii) synergistic bioactivity of the phytochemical capping layer from *C. scabiosus* [4, 11, 13]. The 10–20 nm primary particle size confirmed by DLS and HRTEM provides an enhanced reactive surface area for these bactericidal interactions.

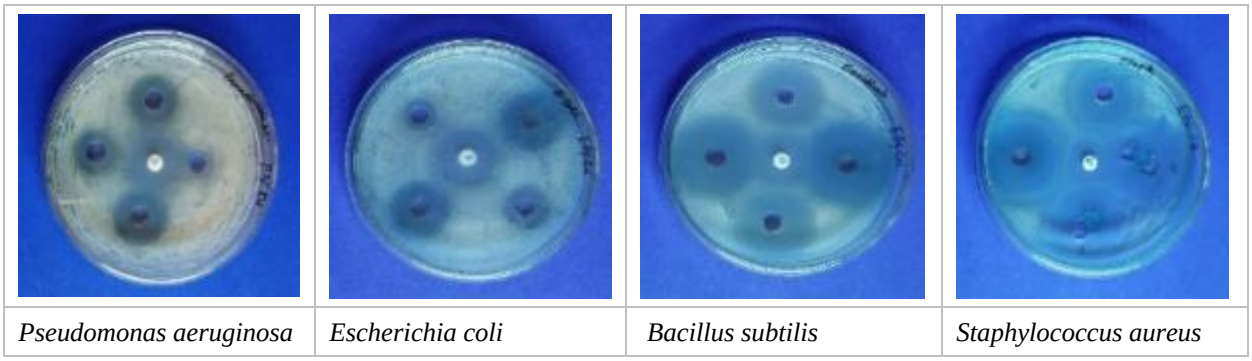

Pseudomonas aeruginosa	*Escherichia coli*	*Bacillus subtilis*	*Staphylococcus aureus*

Figure 9 Antibacterial activity of CuONPs from C. scabiosus Fruit extract through Agar well-diffusion method

The antifungal potential of CuONPs was evaluated against the phytopathogens *Aspergillus niger, Fusarium oxysporum, Macrophomina phaseolina,* and *Sclerotium rolfsii* (Table 2). At 20 µg/mL, moderate inhibition was observed against *F. oxysporum* (50% inhibition) and slight inhibition against *M. phaseolina. A. niger* and *S. rolfsii* showed resistance at lower concentrations. The incomplete inhibition of some phytopathogens may reflect the higher cell wall complexity of filamentous fungi relative to yeasts and bacteria. Further quantitative MIC studies at higher concentrations are warranted to fully characterize the antifungal spectrum of these CuONPs.

Table 2 Antifungal activity of Cu NPs against phytopathogenic fungi

Conc. (µg/mL)	***A. niger***	***F. oxysporum***	***M. phaseolina***	***S. rolfsii***
20	–	50% inhibition	Slight inhibition	–
40	–	–	–	–
60	–	–	–	–
80	–	–	–	–
Standard	–	–	–	–

4. Conclusion

The present study successfully demonstrates the green synthesis of CuONPs using the aqueous fruit extract of the endemic and IUCN Vulnerable species *Croton scabiosus* Bedd. (Euphorbiaceae). The fruit extract served as both oxidizing

and capping agent, converting $Cu^{+}2$ ions to CuO through mild oxidative biosynthesis. Comprehensive characterization confirmed: (i) UV absorption at 274 nm with band gap 2.65 eV (UV–Vis); (ii) Cu–O lattice vibrations with phytochemical capping (FTIR); (iii) simple cubic crystalline phase, crystallite size 10–20 nm (XRD); (iv) elemental purity 62.58 wt% Cu, 37.42 wt% O (EDX); (v) porous agglomerated morphology with primary particles 217–508 nm (SEM); (vi) spherical primary nanocrystallites 10–20 nm with polycrystalline SAED rings (HRTEM); (vii) mean hydrodynamic diameter 19.3 nm, PDI 0.329 (DLS); and (viii) zeta potential −13.2 mV (HORIBA SZ-100).

The CuONPs exhibited: potent antibacterial activity (max ZOI 42 ± 0.1 mm for S. aureus at 200 μg/mL, exceeding gentamicin); antifungal activity against phytopathogens. These results establish C. scabiosus-mediated CuONPs as highly promising nanomaterials for antimicrobial - pharmaceutical applications. Future work should be warranted to determine the complete potential and usage of these bio-synthesized CuONPs.

Compliance with ethical standards

Acknowledgments

The authors express sincere gratitude to the Department of Botany & DST-PURSE Science Centre, Sri Venkateswara University, Tirupati, STIC-SAIF centre, Kochi, Cochin University for supporting lab work. The authors thank the forest authorities of Y.S.R. Kadapa District for permission to collect plant material from Polathla Forest Reserve, and Himedia Laboratories for supplying standard microbiological media and reagents.

Disclosure of conflict of interest

The authors declare no conflict of interest.

Statement of ethical approval

This study did not involve human participants or animal experimentations.

Funding

This research received no specific external funding.

References

[1] Bhati M (2021). Biogenic synthesis of metallic nanoparticles: Principles and applications. Materials Today: Proceedings. https://doi.org/10.1016/j.matpr.2021.04.272.

[2] Saini N, and Ledwani L (2022). Potential applications of nanotechnology in agriculture: Conceptions, characteristics, prospects and limitations – A review. Nano World Journal 8(S1): S147-S161.

[3] Alshammari B H, Lashin MM A, Mahmood MA, Al-Mubaddel F S, Ilyas N, Rahman N, et al. (2023). Organic and inorganic nanomaterials: fabrication, properties and applications. RSC Advances 13(20): 13735–13785. https://doi.org/10.1039/D3RA01421E.

[4] Narayanan R, and El-Sayed MA. Effect of catalysis on the stability of metallic nanoparticles: Suzuki reaction catalyzed by PVP Palladium nanoparticles (2003). Journal of American Chemical Society 125(27): 8340–8347. https://doi.org/10.1021/ja035044x.

[5] Salamma S, and Ravi Prasad Rao B. In vitro propagation of Croton scabiosus Bedd. (Euphorbiaceae) an endemic and vulnerable tree species (2014). Journal of Advances in Biotechnology 3(3): 229 – 240. https://doi.org/10.1024297/jbt.v3.i3.5023

[6] Venkataratnam K, and Venkataraju R (2005). Folk medicine used for common women ailments by Adivasis in the Eastern Ghats of Andhra Pradesh. Indian Journal of Traditional Knowledge 4(3):267–270.

[7] Padma Y, Sarojinidevi N, Venkaratnam K, Tirupati Reddy G, and Venkata Raju RR (2016). Herbal/folk remedies used for snakebites by tribals/rural people of Rayalaseema region, Andhra Pradesh, India. Journal of Medicinal Plants Studies 4(2):52–56.

[8] Apriandanu D O, and Yulizar Y (2019). Tinospora crispa leaves extract for the simple preparation method of CuO nanoparticles and its characterization. Nanostructures and Nano-objects 20: 100401. https://doi.org/10.1016/j.nanoso.2019.100401.

[9] Yugandhar P, Vasavi T, Shanmugam B, Uma Maheswari Devi P, Sathyavelu K R, and Savithramma N (2019). Biofabrication, Characterization and evaluartion of photocatalytic dye degradation efficiency of Syzygium alternifolium leaf extract mediated copper oxide nanoparticles. Materials Research Express 6(6): 065034. https://doi.org/10.1088/2053-1591/ab0db9.

[10] Prabu P, and Losetty V (2024). Green synthesis of copper oxide nanoparticles using Macroptilium lathyroides (L) leaf extract and their spectroscopic characterization, biological activity and photocatalytic dye degradation study. Journal of Molecular Structure 1301: 137404. https://doi.org/10.1016/j.molstruc.2023.137404.

[11] Balaji T, Manushankar C M, Al-Ghanim K A, Kamaraj C, Tirumurugan D, Tanigaivel S, et al. (2023). Padina boergesenii-mediated copper oxide nanoparticles synthesis, with their antibacterial and anticancer potential. Biomedicines 11(8): 2285. https://doi.org/10.3390/biomedicines11082285.

[12] Renuga D, Jeyasundari J, Shakthi Athithan AS, and Arul Jacob YB (2020). Synthesis and characterization of copper oxide nanoparticles using Brassica oleracea var. italic extract for its antifungal application. Materials Research Express 7(4): 045007. https://doi.org/10.1088/2053-1591/ab7b94.

[13] Elango B, Okram G S, and Mathanmohun M. Pharmacological applications of plant-mediated synthesized nanomaterials. Current Pharmacological Reports 9: 511–522. https://doi.org/10.1007/s40495-023-00340-0.

[14] Duan X J, Zhang W W, Li X M, and Wang B G (2006). Evaluation of antioxidant property of extract and fractions obtained from a red alga, Polysiphonia urceolata. Food Chemistry 95(1): 37–43. https://dx.doi.org/10.1016/j.foodchem.2004.12.015.

[15] Ahmed SS, and MR K (2023). Elucidation of antidiabetic mechanism of Centella asiatica and Zingiber officinale — an in vitro and in vivo approach. Journal of Research in Pharmacy 27(1): 420–431. http://dx.doi.org/10.29228/jrp.324.

[16] Jeyabaskar S, Viswanathan T, Radha M, Rathisre P R, and Nishandhini M (2017). Comparative quantitative screening of secondary phytoconstituents from the leaves extracts of Sterculia foetida Linn. Research Journal of Pharmacy and Technology 10(9): 2907-2912. https://doi.org/10.5958/0974-360X.2017.0051.3.

[17] Bauer A W, Kirby W M, Sherris J C, and Turck M (1966). Antibiotic susceptibility testing by a standardized single disk method. American Journal of Clinical Pathology 45(4):493–496.

[18] Balouiri M, Sadiki M, and Ibnsouda S K (2016). Methods for in vitro evaluating antimicrobial activity: A review. Journal of Pharmaceutical Analysis 6(2): 71–79. https://doi.org/10.1016/j.jpha.2015.11.005.